Progress In Electromagnetics Research C, Vol. 130, 95–105, 2023

Performance Enhancement of Patch Antenna Using RIS and Metamaterial Superstrate for Wireless Applications

Swapna K. Budarapu[1, *], M. Shyam Sunder[1], and Bollapragada Ramakrishna[2]

Abstract—This paper proposes a single feed circularly polarised patch antenna with reactive impedance surface (RIS) and metamaterial superstrate (MS) to improve bandwidth and gain for Wi-Fi and Wi-Max applications that demand high gain, wide band, and directional antennas. In this paper, we demonstrate the performance of several antenna designs, including a slot-loaded patch on a single substrate, an antenna on a dual layer substrate with RIS, and an antenna with RIS and MS. The cavity formed by the superstrate and antenna ground plane functions as a Fabry-Perot resonator (FPR) that enhances bandwidth and gain simultaneously. The final optimised antenna has a significantly wider impedance bandwidth (IBW) of 17.32% (5.01 GHz–5.96 GHz) and an axial ratio bandwidth (ARBW) of 6.29% (5.23 GHz–5.57 GHz) than the conventional slot loaded patch antenna. The proposed antenna gain is 11.73 dB, which is around 9 dB increase over the gain of a standard antenna.

1. INTRODUCTION

The demand for low cost, power-efficient, and portable system designs has increased as a result of the expanding number of wireless applications. Modern wireless systems require extremely fast data transfer rates. To get such data rates, antennas must have a number of distinctive characteristics, such as wide bandwidth, high gain, small size, light weight, and ease of integration with microwave circuits. Although microstrip patch antennas (MPAs) often meet the standards of light weight and compactness, their use in some systems is limited due to narrow bandwidth, poor gain, and low efficiency. An effective antenna should have a high gain, hence it can use less power and can transmit to great distances. The antenna's IBW should be wider in order to transmit all frequency bands while maintaining optimal radiation patterns in the broadside direction. MPAs have a small bandwidth and a directional radiation pattern that radiates in the broadside direction. Circular polarization (CP) makes signal transmission independent of how the transmitting and receiving antennas are oriented, and it is preferred over linear polarization (LP). Faraday's rotation causes LP waves to modify the polarization in the atmosphere, whereas CP waves retain the same polarization.

A variety of approaches for improving bandwidth have been reported in the literature, including thick low permittivity substrates, stacked patches, and parasitic elements. A microstrip patch antenna's bandwidth increased by using a thick substrate is presented in [1]. A slot coupled stacked patch antenna is proposed to increase bandwidth in [2]. In [3], a wideband antenna is made using the space between the patches, and circular polarisation is achieved using truncated corners of the patches. Because the antenna height is so high in these structures, the antenna volume is increased. As a result, to address these challenges, high impedance surfaces (HISs) [4] and artificial ground structures (AGSs) [5] are used. A truncated corner square patch with artificial ground structures is proposed to improve impedance bandwidth and achieve circular polarization in [6].

Received 26 November 2022, Accepted 7 February 2023, Scheduled 21 February 2023

* Corresponding author: Swapna Kumari Budarapu (swapnakumaribudarapu@gmail.com).

[1] University College of Enginnering, Osmania University Hyderabad, Telangana, India. [2] Scientist-F, DLRL, DRDO, Hyderabad, India.

Several methods for increasing gain have already been described in the literature, including antenna arrays, surface-mounted horn antennas, antenna hybridization, partially reflecting surface (PRS), and photonic band gap (PBG). Array antenna elements are an efficient approach to increase antenna gain [7, 8]. However, the drawback of this approach is the coupling between elements and the use of power source for each antenna. Other options, such as using substrates with high permittivity or permeability, have also been proposed [9]. The gain enhancement of rectangular patch by surface mounting horn antenna is presented in [10]. A lens antenna is used for gain enhancement in [11]. The above mentioned methods are bulky, expensive, and suffer from surface waves, which influence the antenna's main properties such as emission pattern.

Fabry-Perot resonator antennas are the most commonly used technology for increasing antenna performance while reducing cost and design complexity. In the FPR, the ground plane and superstrate form a cavity. Superstrates of many types are used, such as frequency selective surfaces (FSSs), partially reflecting surfaces (PRSs), and metamaterials.

Metamaterials are artificially engineered materials with unusual electromagnetic properties [12]. These novel artificial materials are made up of periodic unit cell structures that are placed into a material, allow some extraordinary characteristics that are not possible to produce with materials available in nature. Particularly, the permittivity and permeability are both negative which implies negative refractive index and leads to potential applications. Perfect lensing [13], cloaking [14], and miniaturization of microwave devices [15] are a few examples. The method for increasing the antenna gain is to cover it with a MS. A high gain slotted microstrip patch antenna with Meta surface is presented in [16]. An FPR antenna with high gain and high aperture efficiency is presented using MS [17]. A gain improvement of a patch antenna employing a dielectric holey superstrate is presented [18]. In [19], the authors proposed a high gain circularly polarized rectangular patch antenna made of zero index metamaterial (ZIM). The methods for simultaneous increase in antenna bandwidth and gain are provided in [20–23].

This work presents a high gain, wideband antenna composed of a slot-loaded patch antenna, a metamaterial superstrate layer, and a reactive impedance surface (RIS). When a normal antenna is combined with a metamaterial layer and RIS, it behaves like an FPR, and both gain and bandwidth are improved concurrently. The antenna design is simulated using the High-Frequency Structure Simulator (HFSS), and measurements are taken in an anechoic chamber. It is observed that measured results are nearly identical to simulated ones.

The following is how the paper is organized. In Section 2, the designs of a conventional antenna, tan antenna with RIS structure arrangement, an antenna with metamaterial superstrate and RIS arrangement, and their results are discussed. Section 3 compares the measured results of fabricated antenna and simulated results.

2. DESIGN OF ANTENNA AND METASURFACE PERFORMANCE

2.1. Slot-Loaded Patch Antenna Design

Slot-loaded patch antennas provide better performance than other common patch structures such as square, round, and rectangle structures. The geometry of a slot loaded antenna is shown in Fig. 1. Other conventional constructions require many feeds to achieve circular polarization, but a slot loaded patch antenna requires only one feed. The feed location of the antenna is optimized to produce two orthogonal fields, resulting in circular polarisation. The slot loaded patch is printed on an FR4 substrate, and the bottom layer of substrate serves as a ground. An SMA (Sub-Miniature version A) connector provides probe feeding. The SMA inner connector is attached to the slotted patch, while SMA outer connector is attached to ground. The finite element method (FEM) in HFSS is used to create this antenna design. From the simulation results (Fig. 2) the impedance bandwidth is 7.84% (5.39 GHz–5.83 GHz); the gain is 3 dB; and the axial ratio is 1.09% (5.47 GHz–5.53 GHz). The substrate is considered to be sufficiently large to support the gain and bandwidth changes.

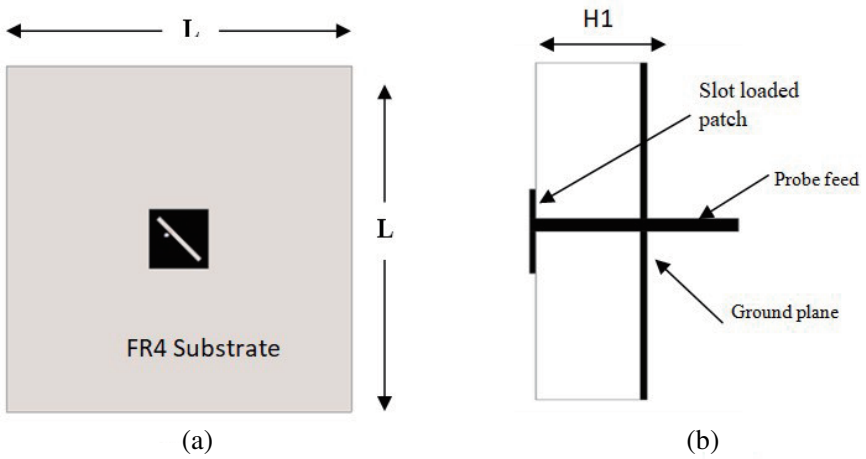

Figure 1. The slot loaded conventional patch antenna. (a) Top view. (b) Side view.

2.2. Slot Loaded Patch Antenna on RIS Structure

An antenna's bandwidth and radiation properties can be greatly improved by using a RIS as the substrate for planar antennas, which can significantly decrease the size of antenna [24]. RIS can store magnetic or electric energy, which can then be used to compensate for the electric or magnetic energy stored beneath the antenna, resulting in antenna miniaturization and bandwidth increase. When RIS is used as the ground plane of a microstrip antenna, the magnetic energy stored in the RIS below the resonance frequency cancels the stored electric energy in the near field (inside dielectric) of the microstrip patch. This causes the microstrip patch to resonate at a lower frequency than its theoretical resonance, indicating antenna miniaturization.

A RIS surface is placed between the patch and the ground plane to improve the IBW of the proposed slot-loaded patch antenna. A RIS surface is printed at the intersection of the two substrates, or on top of the lower layer. RIS patch size and patch count are two characteristics that influence impedance matching. An array of $6 * 6$ square RIS elements is placed on top of the FR4 substrate after the RIS patch size and array size are adjusted. The square patch dimension (L_r), periodicity (p), substrate height (H_1), and substrate height (H_2) are all parametrically analysed. L_r, p, H_1, and H_2 are tuned at 5 mm, 6.2 mm, 1.6 mm, and 0.8 mm, respectively, for broad bandwidth.

The electric field in the broadside direction can be calculated by adding the directly transmitting wave E_t and the reflected wave of the RIS surface E_r:

$$E = E_t + E_r \tag{1}$$

$$E_t = \frac{E_0}{2}(X + Y)e^{-jkz} \tag{2}$$

$$E_r = \frac{E_0}{2}\left(Xe^{-2jkh+\theta_x} + Ye^{-2jkh+\theta_y}\right)e^{-jkz} \tag{3}$$

where E_0 is the magnitude of the electric field component, k the wavenumber, h the antenna height above the ground plane, θ_x the incident wave phase polarised along the X direction, and θ_y the incident wave phase polarised along the Y direction. In this case, the antenna is very close to the ground plane, and $2kh$ is nearly zero in Equation (3). The RIS surface is chosen to have appropriate polarization dependent reflection phases, $\theta_x = -90°$ and $\theta_y = 90°$.

$$E = \frac{E_0}{2}((X + Y) - j(X - Y))e^{-jkz} \tag{4}$$

According to Equation (4), the RIS surface converts a linearly polarised wave into a circularly polarised wave. The impedance bandwidth of 12.15% (5.10 GHz–5.76 GHz) is attained after optimising the RIS structure, as illustrated in Fig. 5. The RIS approach has increased bandwidth. The ARBW is 2.28% (5.20 GHz–5.32 GHz). However, there is no significant change in antenna gain, as shown in Fig. 2.

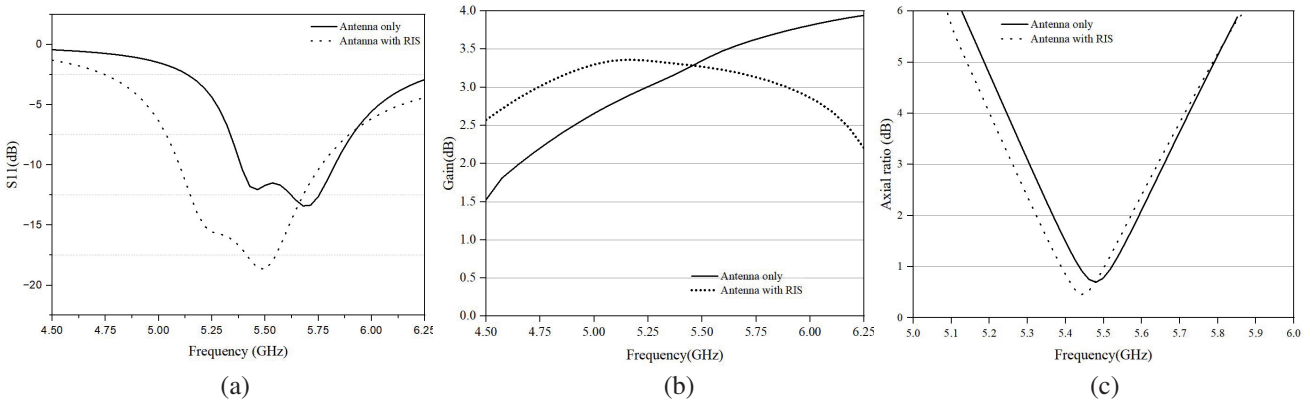

Figure 2. Simulated results of antenna only and antenna with RIS. (a) Reflection coefficient S_{11}. (b) Gain. (c) Axial ratio.

2.3. Performance of Metamaterial Superstrate

The metamaterial superstrate employed in this paper was built using a split ring resonator (SRR), which was introduced first in 1999 [25] by Pendry et al. to produce negative permeability in a specific frequency band. The geometry, size, and location of the metamaterial all have an effect on the antenna's performance. The various parameters that decide the resonant frequency of SRR are split width, gap distance, and metal width. A current flows from one ring to the next via the inter-ring spacing, when the SRR is exposed to an external magnetic field, and the structure acts as an oscillating L-C circuit.

Figure 3 shows the geometry of an SRR unit cell, whereas Fig. 5 depicts a geometric schematic of a metamaterial superstrate composed of an array of this SRR. The geometrical dimensions of the SRR unit cell are as follows: radius of outer split ring $(R1) = 4.5\,\text{mm}$, split gap $(g) = 0.5\,\text{mm}$, width of split rings $(w) = 1.5\,\text{mm}$, and distance between inner and outer rings $(s) = 0.5\,\text{mm}$. SRR's dimensions are designed such that its total length is less than $\lambda/10$, resulting in the particle acting as a subwavelength element.

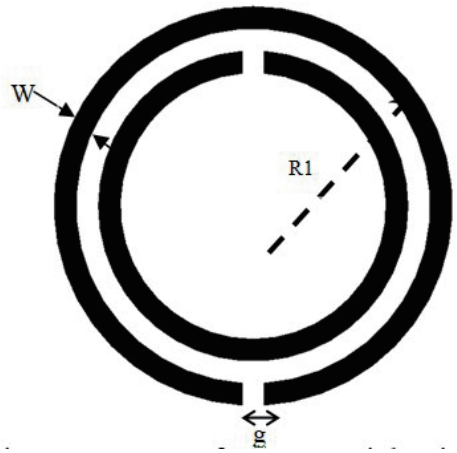

Figure 3. Geometry of metamaterial unit cell.

The effective permeability of the SRR unit cell is calculated using the Nicolson-Ross-Weir (NRW) method [26]. The metamaterial properties of the SRR unit cell are validated using the unit cell simulation S-parameters and MATLAB code. The reflection coefficient magnitude grows towards 0 dB, i.e., unity (Fig. 4(a)), and the reflection coefficient phase is near 180° (Fig. 4(b)) over the required frequency range to meet the requirements of a highly reflective superstrate for gain improvement.

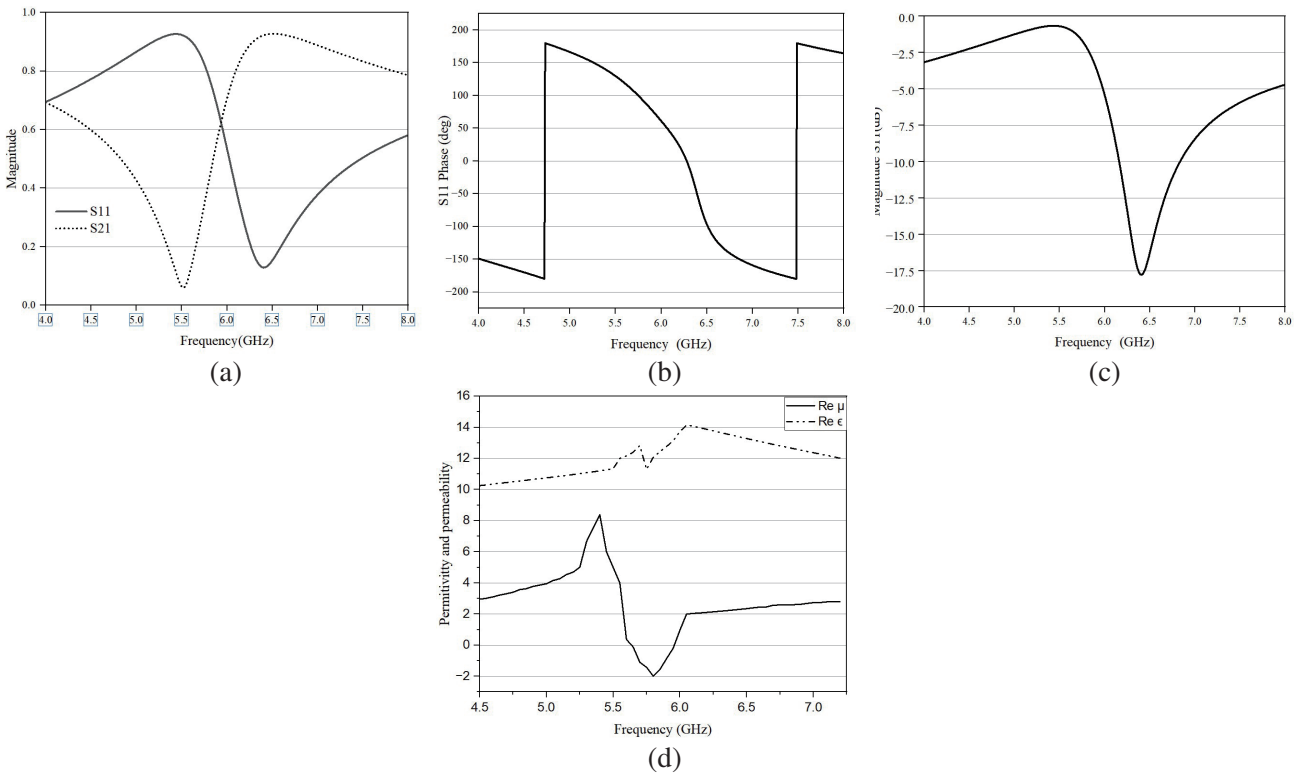

Figure 4. (a) Magnitude of reflection and transmission coefficients. (b) Phase of reflection coefficient. (c) Reflection coefficient S_{11}. (d) Permittivity and permeability of unit cell.

As demonstrated in Fig. 4(d), the unit cell structure possesses negative permeability, indicating that it has metamaterial qualities and no negative permittivity. When the MS superstrate is placed at approximately half-wavelength height from the antenna, it generates an air-filled cavity between the superstrate and ground plane. When a highly reflective superstrate is placed at an optimal height from the antenna, electromagnetic rays are focused along the transmitting direction and generate concentrated rays in the broadside direction, improving antenna gain. It is generally known that raising the value of the reflection coefficient to unity increases directivity (0 dB).

2.4. Antenna with RIS and Metamaterial Superstrate Configuration

The antenna proposed in this paper is made up of a slotted patch antenna, an MS, and a RIS structure. As shown in Fig. 5, the RIS structure is positioned beneath the slot-loaded patch antenna, while the metamaterial superstrate is positioned above the antenna. The cavity generated by the metamaterial superstrate and the antenna ground plane serves as an FPR [27]. The cavity collects both transmitted and reflected rays from the patch antenna. The broadside direction is emitted by the coherent accumulation of trapped rays. As a result, the antenna's gain increases significantly. The proposed antenna with RIS structure and MS is modelled in HFSS, and the resulting simulated results are shown in Fig. 6.

As shown in Fig. 6(a), the impedance bandwidth is 17.32% (5.01 GHz–5.96 GHz), with a 9.5% improvement. The antenna gain is 11.73 dB, as shown in Fig. 6(b), with a gain improvement of approximately 9 dBi. Table 1 compares the proposed antenna performance findings to conventional antenna performance results.

It is found that the antenna with a RIS structure enhances IBW significantly. However, as seen in Fig. 6(b), there is no noticeable increase in gain. The conventional antenna with a RIS structure and an MS improves both bandwidth and gain, as demonstrated in Figs. 6(a), (b), and (c).

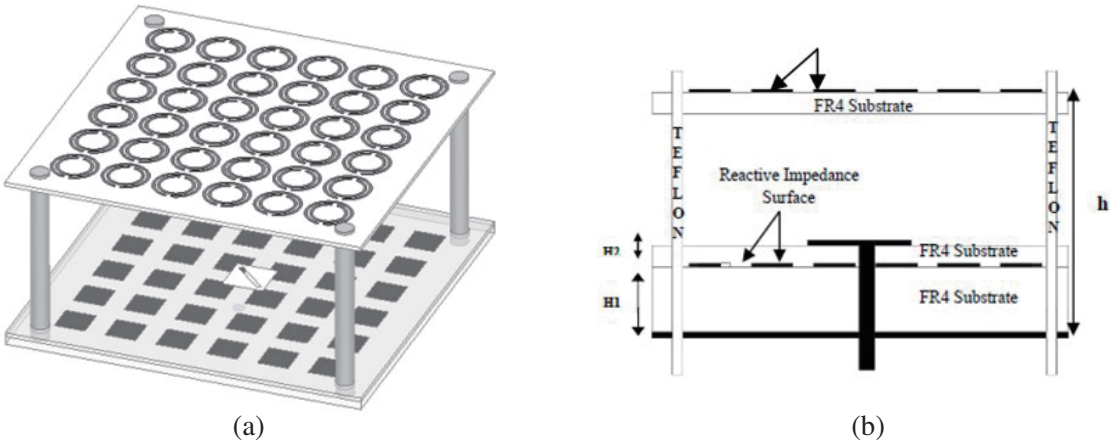

Figure 5. A slot loaded patch antenna with RIS and MS. (a) 3D view. (b) Geometry (front view).

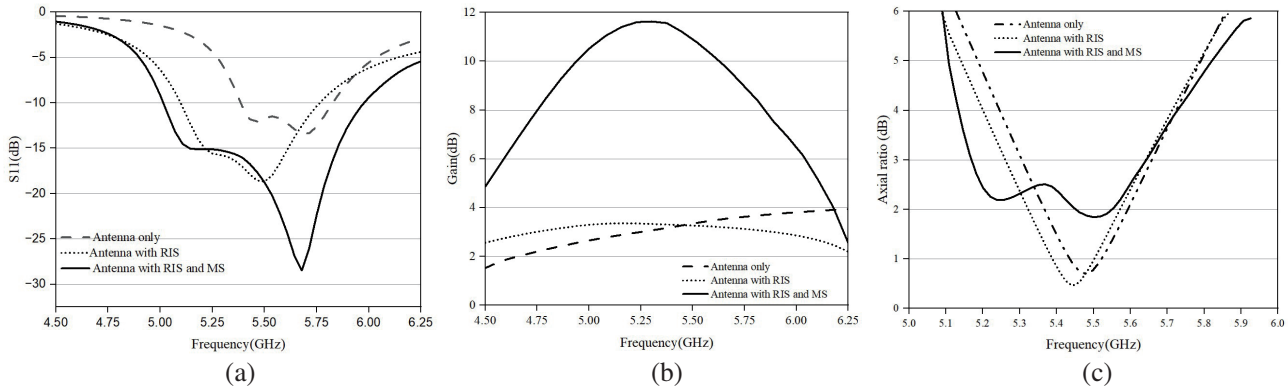

Figure 6. Simulated results of antenna only, antenna with RIS, antenna with RIS and MS. (a) Reflection coefficient S_{11}. (b) Gain. (c) Axial ratio.

Table 1. Comparision of results of conventional antenna, antenna with RIS, antenna with RIS and MS at $h = 31.5\,\text{mm}$.

S. No	Antenna	IBW	Gain (dB)	AR bandwidth
1	Slot loaded patch antenna	7.84% (5.39 GHz–5.83 GHz)	3	1.09% (5.47 GHz–5.53 GHz)
2	Slot loaded patch with RIS structure	12.15% (5.10 GHz–5.76 GHz)	4	2.28% (5.20 GHz–5.32 GHz)
3	Slot loaded patch with RIS and metamaterial superstrate	17.32% (5.01 GHz–5.96 GHz)	11.73	8.5% (5.18 GHz–5.64 GHz)

As illustrated in Fig. 7, the proposed antenna surface current density vector on the patch rotates counterclockwise as the phase increases, indicating that the antenna is right hand circularly polarized (RHCP). As shown in Fig. 8, the RHCP gain is high over the complete bandwidth, but the left hand circularly polarized (LHCP) gain is −12 dB at 5.2 GHz, where the antenna needs to maintain circular polarization.

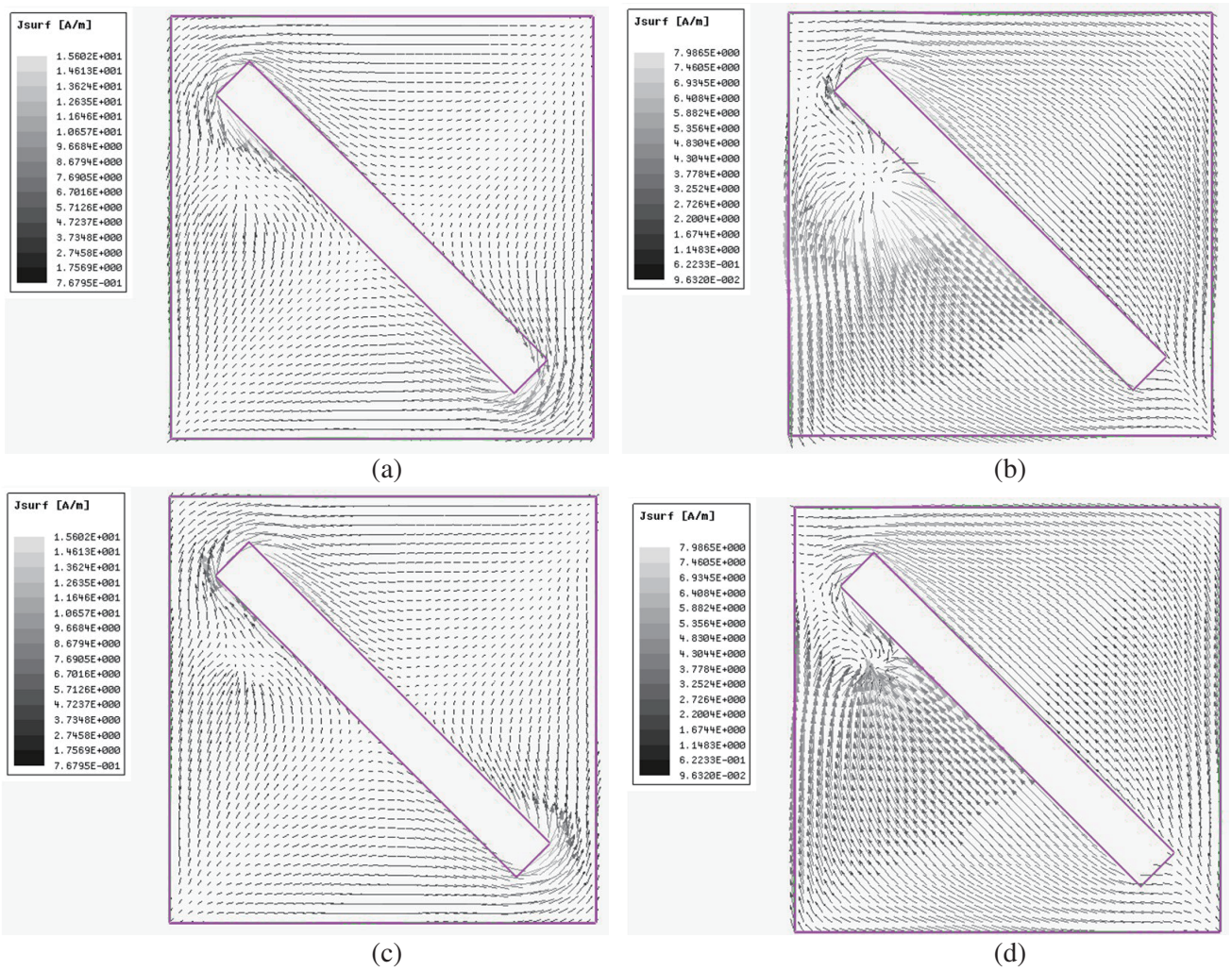

Figure 7. Antenna with RIS and MS surface current density vector on slot loaded patch at 5.3 GHz. (a) Phase = 0°, (b) Phase = 90°, (c) Phase = 180°, (d) Phase = 270°.

Table 2 compares the proposed antenna findings to those reported in the literature. We can see that the proposed antenna planar size ($1\lambda_0 * 1\lambda_0$) is quite small in comparison to other antennas, and the superstrate is situated at a distance of half wavelength height ($\approx \lambda_0/2$).

3. FABRICATION AND MEASURED RESULTS OF PROPOSED ANTENNA

The slot loaded patch antenna, RIS structure, and MS are all built on an FR4 substrate. The MS is positioned approximately half a wavelength above the radiating patch using Teflon rods, as seen in Fig. 9. The usage of Teflon rods has no effect on the antenna's radiating properties. The suggested antenna's reflection coefficient (S_{11}) is tested with a network analyzer in the frequency range of 4.5 GHz to 6.25 GHz, as shown in Fig. 10(a). The gain of an antenna is assessed using the gain transfer method, which employs a standard gain horn antenna with known gain. As shown in Fig. 10(b), the measured and simulated gains are nearly identical. Due to fabrication errors, there is a minor difference between measured and simulated values. At frequencies of 5.25 GHz and 5.9 GHz, Fig. 11 compares the radiation patterns of the fabricated antenna and simulated antenna.

Table 2. Comparison of proposed antenna performance with published literature.

S. No	Reference	Frequency range (GHz)	Height of substrate (mm)	Gain (dB)	Impedance bandwidth (%)	Axial ratio (%)	Planar size
1	5	14.9–15.3	$\approx \lambda_0/2$	21	2.5%	7%	$7\lambda_0 * 7\lambda_0$
2	6	9.85–10.1	$\approx \lambda_0/2$	15	2.3%	0.6%	$2.758\lambda_0 * 2.758\lambda_0$
3	7	11.7–19.8	$\approx \lambda_0/2$	11.5	54%	29%	$1.75\lambda_0 * 1.75\lambda_0$
4	8	29.1–31.6	$\approx \lambda_0/2$	15.2	9.6%	2.67%	$2.50\lambda_0 * 2.50\lambda_0$
5	16	9.24–11.25	$\approx \lambda_0/2$	7.57	7.66%	-	$0.9\lambda_0 * 0.9\lambda_0$
6	17	8.2–11	Greater than $\lambda_0/2$	12.5	5%	-	$2.88\lambda_0 * 2.88\lambda_0$
7	18	5.71–5.87	$\approx \lambda_0/2$	6.8	2.7%	-	$1.2\lambda_0 * 1.2\lambda_0$
8	19	7.11–7.56	$\approx \lambda_0/2$	12.31	6.87%	6.87%	$2.09\lambda_0 * 2.09\lambda_0$
9	Proposed work	5.01–5.96	$\approx \lambda_0/2$	11.73	17.32%	8.5%	$1\lambda_0 * 1\lambda_0$

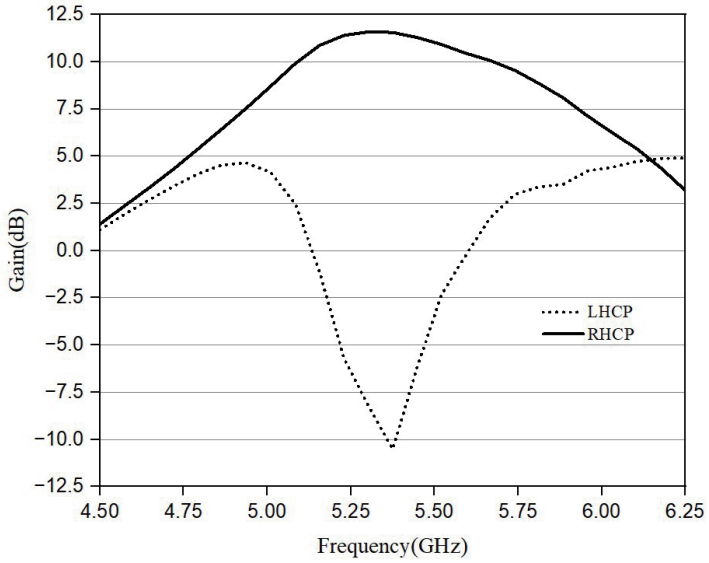

Figure 8. Simulated LHCP and RHCP gain of proposed antenna.

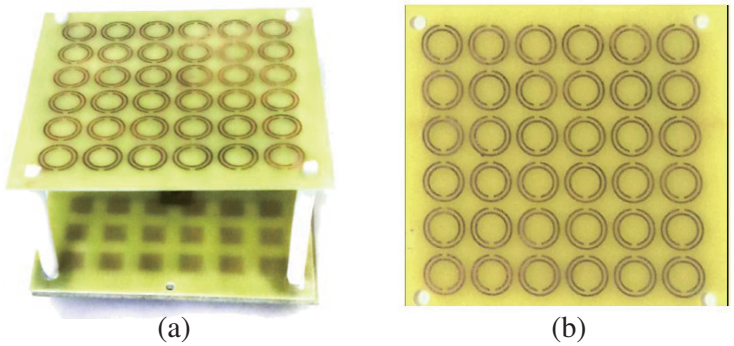

Figure 9. (a) Fabricated antenna with RIS and MS. (b) Metamaterial superstrate.

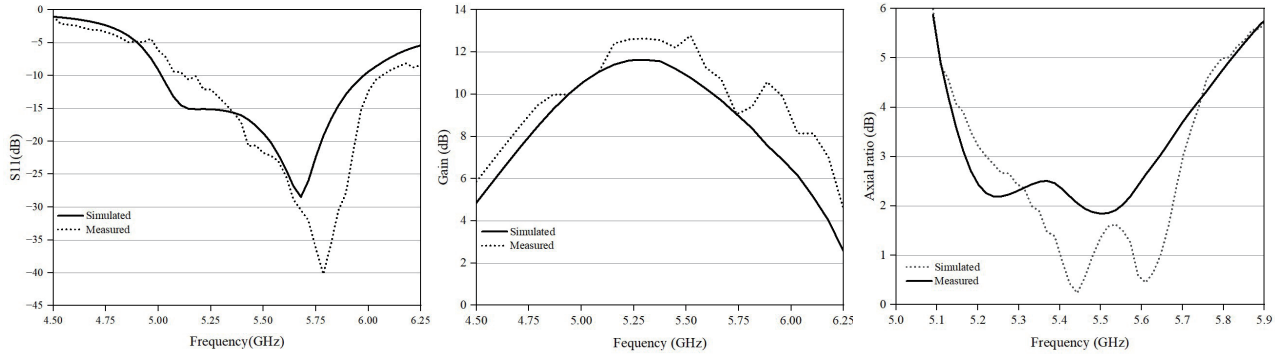

Figure 10. Simulated and measured results of proposed antenna with RIS and MS. (a) Reflection coefficient (S_{11}). (b) Gain. (c) Axial ratio.

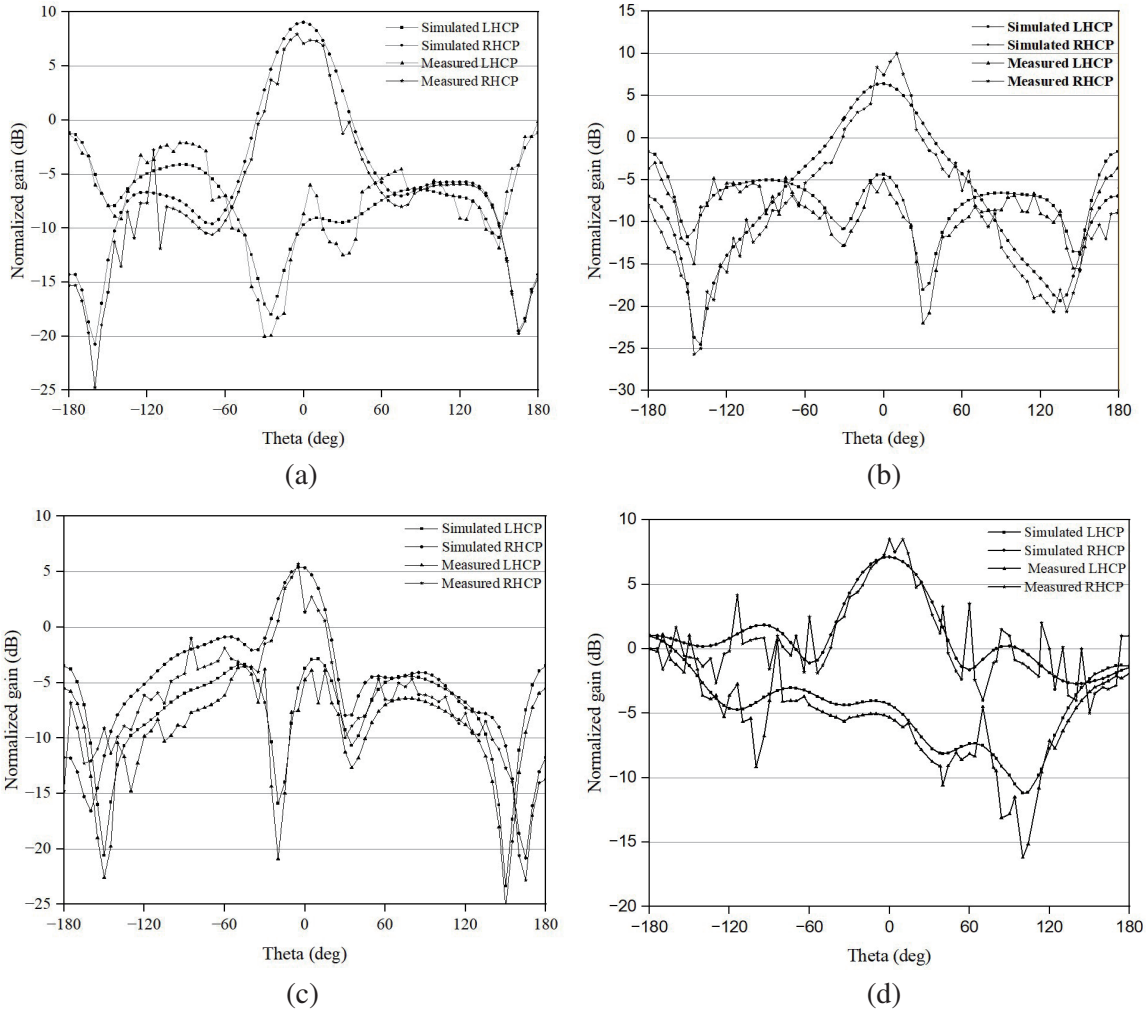

Figure 11. Simulated and measured radiation patterns of proposed antenna at 5.25 GHz. (a) $\phi = 0$, (b) $\phi = 90$ and at 5.9 GHz, (c) $\phi = 0$, (d) $\phi = 90$.

4. CONCLUSION

A circularly polarized slot loaded patch antenna with high gain and broad bandwidth is designed. The properties of metamaterial unit cell are investigated. The IBW and gain of a standard patch antenna are improved by adding a RIS structure as the ground plane and a metamaterial surface as the superstrate. The slot-loaded patch with RIS and MS works as an FPR. The gain of the designed antenna is 11.73 dB, which is about 9 dB higher than the gain of the conventional antenna. The designed antenna's IBW is 17.32% (5.01 GHz–5.96 GHz), which is 9.5% more than the typical antenna BW. The proposed antenna radiates CP waves, with an ARBW of 6.29% (5.23 GHz–5.57 GHz) for AR $<$ 3 dB. The proposed antenna is fabricated and tested to validate the simulation results. The comparison of the performance of conventional and proposed antennas shows that metamaterials have a considerable potential for improving antenna parameters. The proposed antenna can be used for Wi-Fi and Wi-Max applications, based on the simulated and measured results.

ACKNOWLEDGMENT

The authors would like to thank Director, DLRL, DRDO, Hyderabad.

REFERENCES

1. Kovitz, J. M. and Y. Rahmat-Samii, "Using thick substrates and capacitive probe compensation to enhance the bandwidth of traditional cp patch antennas," *IEEE Transactions on Antennas and Propagation*, Vol. 62, No. 10, 4970–4979, 2014.
2. Serra, A. A., P. Nepa, G. Manara, G. Tribellini, and S. Cioci, "A wide-band dual-polarized stacked patch antenna," *IEEE Antennas and Wireless Propagation Letters*, Vol. 6, 141–143, 2007.
3. Kim, S. M. and W. G. Yang, "Single feed wideband circular polarised patch antenna," *Electronics Letters*, Vol. 43, No. 13, 1, 2007.
4. Sajin, G. I., "Impedance measurement of millimeter wave metamaterial antennas by transmission line stubs," *Progress In Electromagnetics Research Letters*, Vol. 26, 59–68, 2011.
5. Zhang, Y., J. Von Hagen, M. Younis, C. Fischer, and W. Wiesbeck, "Planar artificial magnetic conductors and patch antennas," *IEEE Transactions on Antennas and Propagation*, Vol. 51, No. 10, 2704–2712, 2003.
6. Nakamura, T. and T. Fukusako, "Broadband design of circularly polarized microstrip patch antenna using artificial ground structure with rectangular unit cells," *IEEE Transactions on Antennas and Propagation*, Vol. 59, No. 6, 2103–2110, 2011.
7. Ghassemi, N. and K. Wu, "High-efficient patch antenna array for e-band gigabyte point-to-point wireless services," *IEEE Antennas and Wireless Propagation Letters*, Vol. 11, 1261–1264, 2012.
8. D.-Y. Kim, Y. Lim, H.-S. Yoon, and S. Nam, "High-efficiency W-band electroforming slot array antenna," *IEEE Transactions on Antennas and Propagation*, Vol. 63, No. 4, 1854–1857, 2015.
9. Esselle, K., A. K. Verma, et al., "Compact circularly polarized enhanced gain microstrip antenna on high permittivity substrate," *2005 Asia-Pacific Microwave Conference Proceedings, IEEE*, Vol. 4, 4, 2005.
10. Methfessel, S. and L.-P. Schmidt, "Design of a balanced-fed patch-excited horn antenna at millimeter-wave frequencies," *Proceedings of the Fourth European Conference on Antennas and Propagation, IEEE*, 1–4, 2010.
11. Zhu, H., S. W. Cheung, and T. I. Yuk, "Enhancing antenna boresight gain using a small metasurface lens: Reduction in half-power beamwidth," *IEEE Antennas and Propagation Magazine*, Vol. 58, No. 1, 35–44, 2016.
12. Veselago, V. G., "The electrodynamics of substances with simultaneously negative values of ϵ and μ," *Soviet Physics Uspekhi*, Vol. 10, No. 4, 509, 1968, 1968.
13. Pendry, J. B., "Negative refraction makes a perfect lens," *Physical review letters*, Vol. 85, No. 18, 3966, 2000.

14. Cai, W., U. K. Chettiar, A. V. Kildishev, and V. M. Shalaev, "Optical cloaking with metamaterials," *Nature photonics*, Vol. 1, No. 4, 224–227, 2007.
15. Marqués, R., F. Martin, and M. Sorolla, *Metamaterials with Negative Parameters: Theory, Design, and Microwave Applications*, John Wiley & Sons, 2011.
16. Samantaray, D. and S. Bhattacharyya, "A gain-enhanced slotted patch antenna using metasurface as superstrate configuration," *IEEE Transactions on Antennas and Propagation*, Vol. 68, No. 9, 6548–6556, 2020.
17. Singh, A. K., M. P. Abegaonkar, and S. K. Koul, "High-gain and high-aperture efficiency cavity resonator antenna using metamaterial superstrate," *IEEE Antennas and Wireless Propagation Letters*, Vol. 16, 2388–2391, 2017.
18. Kim, J. H., C.-H. Ahn, and J.-K. Bang, "Antenna gain enhancement using a holey superstrate," *IEEE Transactions on Antennas and Propagation*, Vol. 64, No. 3, 1164–1167, 2016.
19. Rajanna, P. K. T., K. Rudramuni, and K. Kandasamy, "A high-gain circularly polarized antenna using zero-index metamaterial," *IEEE Antennas and Wireless Propagation Letters*, Vol. 18, No. 6, 1129–1133, 2019.
20. Rao, N. and V. D. Kumar, "Gain and bandwidth enhancement of a microstrip antenna using partial substrate removal in multiple-layer dielectric substrate," *Progress In Electromagnetics Research Symposium Proceedings*, 1285–1289, 2011.
21. Attia, H. and O. M. Ramahi, "Ebg superstrate for gain and bandwidth enhancement of microstrip array antennas," *2008 IEEE Antennas and Propagation Society International Symposium*, 1–4, 2008.
22. Nishiyama, E., M. Aikawa, and S. Egashira, "Stacked microstrip antenna for wideband and high gain," *IEE Proceedings-Microwaves, Antennas and Propagation*, Vol. 151, No. 2, 2000.
23. Honari, M. M., A. Abdipour, and G. Moradi, "Bandwidth and gain enhancement of an aperture antenna with modified ring patch," *IEEE Antennas and Wireless Propagation Letters*, Vol. 10, 1413–1416, 2011.
24. Mosallaei, H. and K. Sarabandi, "Antenna miniaturization and bandwidth enhancement using a reactive impedance substrate," *IEEE Transactions on antennas and propagation*, Vol. 52, No. 9, 2403–2414, 2004.
25. Pendry, J. B., A. J. Holden, D. J. Robbins, and W. J. Stewart, "Magnetism from conductors and enhanced nonlinear phenomena," *IEEE Transactions on Microwave Theory and Techniques*, Vol. 47, No. 11, 2075–2084, 1999.
26. Joshi, J. G., S. S. Pattnaik, S. Devi, and M. R. Lohokare, "Frequency switching of electrically small patch antenna using metamaterial loading," *Indian J. Radio Sp. Phys*, Vol. 40, No. 3, 159–165, 2011.
27. Arora, C., S. S. Pattnaik, and R. N. Baral, "Metamaterial inspired DNG superstrate for performance improvement of microstrip patch antenna array," *Progress In Electromagnetics Research B*, Vol. 76, 73–85, 2017.